16th World Conference on Earthquake, 16WCEE 2017
Santiago Chile, January 9th to 13th 2017
Paper N° 0081
Registration Code: S-C1462495181

VARIATION IN SEISMIC PERFORMANCE OF BRIDGES CAUSED BY RIVERBED SCOUR

S.T. Song[(1)], T.F. Hu[(2)] and D.J. Chiou[(3)]

[(1)] *Assistant Professor, National Chung-Hsing University, Taiwan, e-mail: ssong@nchu.edu.tw*
[(2)] *Graduate Research Assistant, National Chung-Hsing University, Taiwan, e-mail: h0425hu@gmail.com*
[(3)] *Graduate Research Assistant, National Chung-Hsing University, Taiwan, e-mail: f25jerry@hotmail.com*

Abstract

This paper applies the capacity spectrum approach to evaluate the seismic performance of a bridge at different scour depths. The capacity spectrum is constructed based on the lateral pushover curve obtained from finite element analysis. During the pushover process, the forces applied on the superstructure and the pile-cap are assessed by the modal analysis of a bridge bent; these forces are adjusted after reaching the yield limit states of the structure to account for the effect of stiffness change. The performance limit of the bridge is identified in the capacity spectrum, and the seismic demand required to reach this performance limit is determined accordingly. The influence of riverbed scour on the seismic performance of a bridge is assessed by comparing the seismic demands correlated to the performance limit at different scour depths. Results highlight that for a bridge originally equipped with sufficient foundation strength, the seismic demand correlated to its performance limit first increases with increasing scour depth. This result indicates an improved seismic performance when the scour depth is shallow. Once the scour depth exceeds a critical level, the seismic performance of the bridge is controlled by the unexpected damages in the foundation. The seismic demand correlated to the performance limit of the bridge decreases, and the seismic performance declines rapidly when the scour depth increases.

Keywords: bridge; multiple hazards; soil-structure interaction; capacity spectrum approach; river scour

1. Introduction

Structures located in regions subjected to multiple natural hazards must be able to withstand the effects of these different hazards. Although multiple natural hazards rarely strike simultaneously, damage caused by one natural disaster can affect the performance of a structure during subsequent hazardous events. Bridge located in flood and earthquake-prone region is one of the notable examples. Rapid water flow during a flood erodes soil around the bridge foundation; this erosion exposes piles after the flood. The loss of surrounding soil reduces the lateral strength and stiffness of the foundation. When a bridge with an exposed pile foundation is subjected to earthquake excitation, the reduced foundation stiffness prolongs the natural vibration period of the bridge and alters the design level seismic demands imposed on the structure. The lateral force from the inertia of the superstructure also induces large flexural demand in the aboveground portion of the pile. In current practice, foundation systems of most bridges are required to have a lateral strength that is greater than the strength of the column. Such a design enables plastic hinges in the column to limit the lateral force imposed on the foundation. Thus, the piles are protected from damage even under severe earthquake excitations. However, for a bridge located in flood and earthquake-prone regions, pile exposure caused by riverbed scour significantly reduces the lateral strength of the foundation. Once the scour depth exceeds a critical level, the strength of the foundation becomes insufficient to prevent unacceptable pile damage caused by an earthquake. Therefore, the seismic performance of a bridge with foundation exposure differs completely from that of the original bridge design without foundation exposure. Given that many bridges in earthquake-prone regions also suffer from serious scour problems, an assessment of the seismic performance of a bridge with foundation exposure is relevant. This assessment can help engineers evaluate the need for foundation retrofitting, particularly to assure a certain level of performance for the structure.

In the present study, the seismic performance of a bridge at different scour depths is assessed by the capacity spectrum approach. The capacity spectrum of the bridge bent is constructed based on the lateral pushover curve obtained by finite element analysis. The finite element model employs fiber beam–column elements to model the reinforced concrete column and piles and the beam-on-nonlinear-Winkler-foundation framework to simulate soil-pile interaction. During the pushover process, the ratio of the incremental lateral force applied on the superstructure to that applied on the pile-cap is determined by the modal analysis of the bridge bent. The lateral force increment is adjusted after the formation of plastic hinges in the structure to account for the effect of significant changes in lateral stiffness. The pushover curve is converted to capacity spectrum following the approach recommended by ATC-40 [1]. A point corresponding to the performance limit of the bridge is identified in the capacity spectrum to ensure the satisfactory seismic performance of the bridge. For a laterally loaded bridge, the inelastic deformations of the foundation must be controlled within the *serviceability* limit; the inelastic deformation of the column cannot exceed the *damage-control* limit. The seismic performance limit of the bridge is defined as either the column or the foundation that first reaches its limit of inelastic deformation. The seismic demand imposed on the structure is assessed using the acceleration–displacement response spectrum, which is constructed considering the hysteretic damping effect from structural yielding. The maximum seismic demand, which the bridge is able to sustain, can be determined when the demand spectrum intersects with the capacity spectrum at the point corresponding to the performance limit of the bridge. In the present study, the influence of riverbed scour on the seismic performance of a bridge is assessed by comparing the maximum allowed seismic demands of the bridge at different scour depths. Considering that the bridge was originally designed with sufficient foundation strength, the results show that its seismic performance is initially governed by the *damage-control* limit of the column. The maximum allowed seismic demand increases with increasing scour depth when the scour depth is shallow. However, once the scour depth exceeds a critical level, the seismic performance of the bridge is governed by the *serviceability* limit of the foundation. Under this limit, the maximum allowed seismic demand decreases as the scour depth increases.

2. Bridge Structure

The type of structure considered in this study is the straight multi-span bridge located in the middle or lower course of a river. This bridge has many spans with a fairly uniform distribution of mass, stiffness, and strength between bents. When subjected to earthquake excitation, the structure may experience a large transverse seismic demand, particularly for the bents around the midway of the bridge. The superstructure stiffness is known to influence the seismic response of the bridge bents. However, the transverse response of the bents around the midway of this type of multi-span bridge remains close to that of an individual bent, because the bridge is long with uniform mass and stiffness distributions. Consequently, the seismic performance of the bridge may be assessed using a single bridge bent subjected to lateral earthquake loads.

A bridge is designed as an example to investigate the influence of riverbed scour on the seismic performance of bridges. The geometry of the bridge bent and the reinforcement details of the column and piles are shown in Fig. 1. The seismic mass of the superstructure is determined from the two adjacent half spans of the superstructure and is equal to $m_s = 700{,}100\ \mathrm{kg}$. The superstructure is supported by a 6-m-tall circular column with a diameter $D_c = 2\ \mathrm{m}$. The centroid of the superstructure is estimated to be 1 m above the tip of the column. The foundation consists of nine 1-m-diameter circular piles ($D_p = 1\ \mathrm{m}$) in a 3 piles × 3 piles arrangement with the center-to-center spacing of piles equal to 3 m ($3D_p$). The pile-cap is an 8 m × 8 m × 2.5 m reinforced concrete block with a mass equal to $m_f = 399{,}100\ \mathrm{kg}$. The bridge columns and piles are assumed to have been carefully detailed with sufficient longitudinal and transverse reinforcements to prevent non-ductile damage. The longitudinal reinforcement of the column is provided by fifty No.43 bars, giving a reinforcement ratio of 2.3%. The transverse reinforcement of the column is provided by No.25 hoop at a pitch of 100 mm. The pile is longitudinally reinforced by twenty No.32 bars with the reinforcement ratio equal to 2%. The transverse reinforcement of the pile is provided by No.19 spiral at 75 mm pitch within the region that is four times the pile diameter from the pile/pile-cap interface. The spacing of the transverse reinforcement is increased to 200 mm for the pile section at larger depths from the pile-head, as shown in Fig. 1. The expected compressive strength of the concrete is taken as $f'_{ce} = 45\ \mathrm{MPa}$. Longitudinal and transverse reinforcements are provided by A706 steel with an expected yield strength of $f_{ye} = 475\ \mathrm{MPa}$. The bridge is assumed to be located at a medium sand site with an effective friction angle of $\bar{\phi} = 35°$; the site is classified as Class D per FEMA-450 [2]. The bridge was originally designed with the piles fully embedded in the riverbed, that is, $L_a = 0$ m . Scouring of the riverbed has caused the bridge to suffer from foundation exposure. In this study, the length of the pile exposure is assumed to vary from $L_a = 0$ m to $L_a = 6D_p$, where $D_p = 1$ m is the pile diameter.

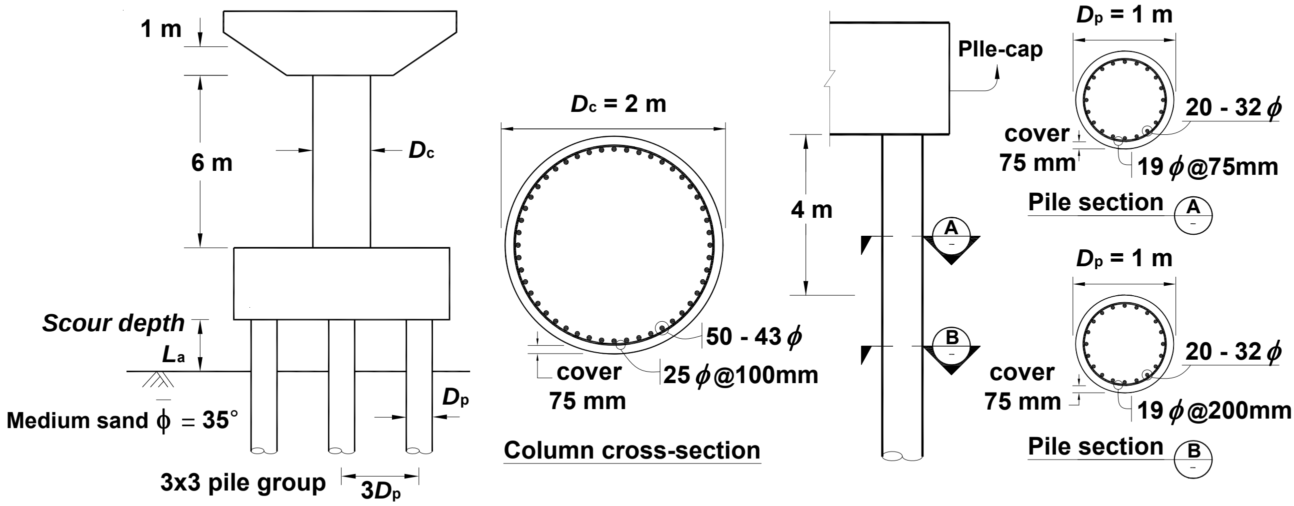

Fig. 1 – Geometry of a bridge bent and the reinforcement details of the column and pile.

3. Capacity Spectrum Approach for Seismic Performance Assessment

3.1 Finite Element Model

The present study uses capacity spectrum method to evaluate the seismic performance of a bridge at different scour depths. The pushover curve to construct the capacity spectrum of the bridge bent is obtained using the 2D nonlinear finite element analysis implemented in the computational platform *OpenSees* [3]. The structure and finite element model of the bridge bent is illustrated in Fig. 2(a). The column and piles are modeled by displacement-based beam–column elements, and the pile-cap is modeled by a series of rigid elements. The cross-section of the elements modeling the reinforced concrete column and piles is discretized into three types of fibers to represent the unconfined concrete cover, confined concrete core, and longitudinal steels. The uniaxial Kent–Scott–Park concrete material model [4] is adopted to describe the stress–strain relations of the confined and unconfined concrete. For the confined concrete core, the compressive strength is calculated based on the model by Mander *et al.* [5] and the ultimate strain is determined according to the equation given in Priestley *et al.* [6]. A modified Menegotto–Pinto model [7] is adopted to define the stress–strain relation of the steel reinforcement. The cross sections of the column and pile elements are shown in Fig. 2(b). Concentrated vertical loads P_s and P_{pc} are applied at the centroid of the superstructure and the centroid of the pile-cap, respectively, to represent the gravity loads from the weights of the superstructure and pile-cap.

The soil-pile interaction for the bridge foundation is modeled based on beam-on-Winkler-foundation framework. Pile elements below the ground level are connected to closely spaced nonlinear springs which represent the lateral soil resistance, as illustrated in Fig. 2(c). The modified API p-y relation proposed by O'Neill and Murchison [8] is used in conjunction with a hyperbolic tangent function to describe the nonlinear resistance of the cohesionless soils. In current practice, pile foundations are commonly constructed with a group of piles, which is subsequently integrated using a heavily reinforced pile-cap. The stiffness and strength of the soil surrounding a pile group are reduced because of the presence of the adjacent piles. Therefore, the stiffness and ultimate resistance given in API soil p-y relation [8] must be multiplied by a group modifier p_m to account for this interaction effect between the soil and the piles. An estimation of the group modifier p_m and its correlation with the center-to-center spacing between piles and the location of the pile in the group are available in Reference [9] and reproduced in Table 1. The group modifier for piles in the leading row of a pile-group is greater than that for piles in the trailing rows. Thus, the soil pressure on the piles in the leading row is more significant. When the model is subjected to lateral loads, structural yielding is first developed in the leading row of the pile group and then sequentially in the trailing rows.

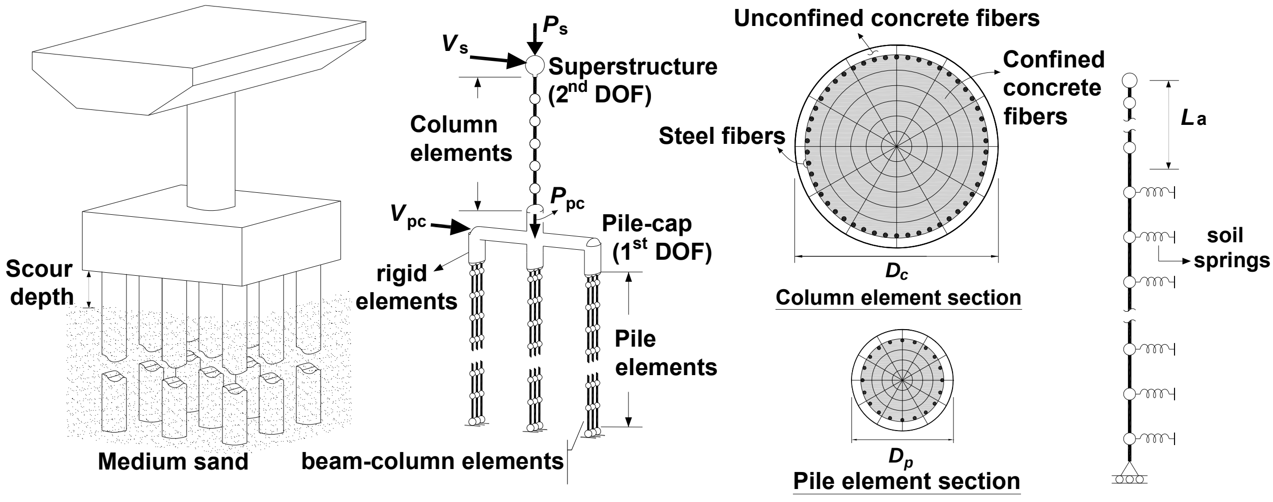

Fig. 2 – Finite element model of the bridge bent.

Table 1 – Group modifier for soil stiffness and strength (adapted from Reference [9])

Pile spacing	Reduction factor, p_m — Piles in the 1st row	Piles in the 2nd row	Piles in the 3rd and subsequent rows
2.0 D_p	0.6	0.35	0.25
3.0 D_p	0.75	0.55	0.4
5.0 D_p	1.0	0.85	0.7
7.0 D_p	1.0	1.0	0.9

Note: (1) The term “row” refers to a line perpendicular to the direction of loading.
(2) 1st row = leading row in lateral movement and 2nd row = 1st trailing row in lateral movement
(3) D_p = pile diameter.

The global capacity of the bridge column and that of the foundation are assessed by the pushover analysis. The load-displacement curves of the column and the foundation are further idealized into a bilinear relation to quantify the design parameters, such as the equivalent stiffness and effective yield strength. The pushover analysis of the column is performed by applying an incremental displacement at the centroid of the superstructure with the pile-cap fully restrained from displacement and rotation. The column is pushed up to a target displacement corresponding to its performance limit, which is defined as the inelastic deformation at the critical section of the column reaching the *damage-control* limit state. Limit strains recommended for the *damage-control* limit state to avoid subsequent replacement of a reinforced concrete column are summarized in Table 2 [10]. The load-displacement curve of the column and its bilinear idealization are plotted in Fig. 3(a). The equivalent elastic stiffness of the column K_{s1} is defined as the secant stiffness through the point corresponding to the first yield of the longitudinal reinforcement. The linear elastic line extends to the point where the lateral force is equal to the strength of the column at its effective yield limit state; this limit state is defined by an extreme fiber compression strain of 0.004 as per the recommendation of Priestley *et al.* [10]. The yield strength of the column is denoted as

V_{Ys} in the present study. The equivalent post-yield stiffness K_{s2} of the bilinear response is determined by equating the area under the nonlinear load-displacement curve to the area under the bilinear idealization. For the bridge column shown in Fig. 1, the elastic stiffness is $K_{s1} = 103747$ kN/m; the post-yield stiffness is $K_{s2} = 2425$ kN/m; and the yield strength is $V_{Ys} = 4626$ kN. The post-yield stiffness K_{s2} of the column is very small compared with the elastic stiffness K_{s1}; this result indicates a nearly plastic behavior of the column after the yield limit state. The load-displacement curve of the foundation before river scouring ($L_a = 0$ m) and its bilinear idealization are shown in Fig. 3(b). The pushover analysis of the foundation is performed by applying an incremental displacement at the centroid of the pile-cap until its performance limit is reached. To prevent any unexpected damage to regions that are not readily assessable, the performance limit of the foundation is defined as the inelastic deformation in the critical section of the piles at the leading row of the pile group reaching its *serviceability* limit state. The recommended strain limits for a reinforced concrete element at the *serviceability* limit state are also summarized in Table 2 [10]. The bilinear load-displacement relation is idealized using an approach similar to what was described above. For a pile group foundation, the first yield point to determine the elastic stiffness K_{f1} is defined by the first yield of the longitudinal reinforcements in the piles at the leading row of the group. The effective yield strength of the foundation V_{Yf} is defined as the piles in the second row of the pile group reaching its yield limit state, which is also defined by an extreme fiber compression strain of 0.004 [10]. The load-displacement curve in Fig. 3(b) shows that the point corresponding to the *serviceability* limit of the foundation is very close to the effective yield limit state. Consequently, the post-yield stiffness of the bilinear idealization should not be determined by equating the area under the nonlinear curve to the area under the idealized curve. In this study, the post-yield stiffness of the foundation K_{f2} is obtained by directly connecting the effective yield limit state in the bilinear idealization to the point of performance limit of the bridge. The elastic stiffness of the foundation with $L_a = 0$ m is $K_{f1} = 317688$ kN/m; the post yield stiffness is $K_{f2} = 58145$ kN/m; and the yield strength is $V_{Yf} = 12918$ kN. Figure 3(b) shows that the foundation still has a significant post-yield stiffness after the yield limit state; the foundation is capable of subjecting a lateral force that is much greater than its yield strength. The lateral stiffness and yield strengths of the column and the foundation are used later to help obtain the load-displacement curve and capacity spectrum of the bridge bent.

Table 2 – Definitions of performance limit states for reinforced concrete sections [10].

Performance limit state	Concrete strain limit	Steel strain limit
Serviceability	$\varepsilon_{cover} = 0.005$	$\varepsilon_s = 0.015$
Damage-control	$\varepsilon_{core} = \varepsilon_{cu}$	$\varepsilon_s = 0.6\varepsilon_{su}$

Note: (1) ε_{cu}: the ultimate strain of confined concrete

(2) ε_{su}: the ultimate strain of reinforcing steel

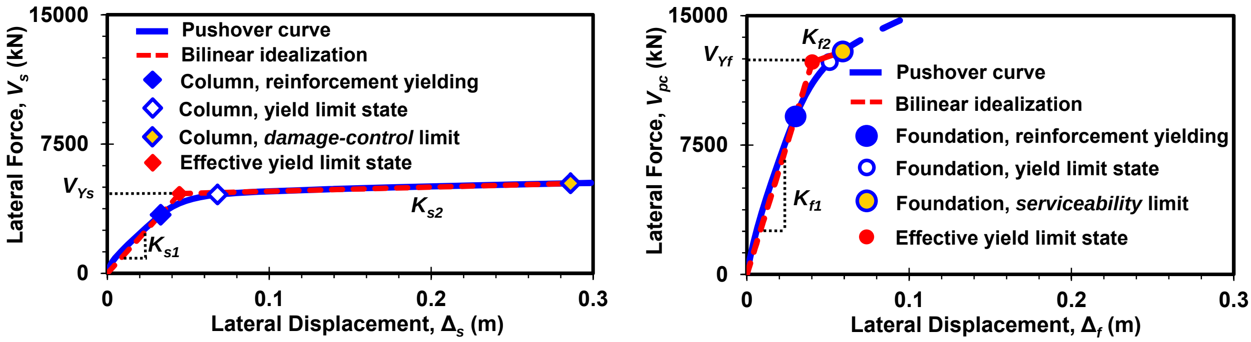

(a) (b)

Fig. 3 – Load-displacement curve and bilinear idealization of (a) column and (b) foundation at $L_a = 0$ m.

3.2 Pushover Analysis of Two-Degree-of-Freedom Bridge Bent

To assess the load-displacement relation of the bridge bent, the bridge is idealized as a two-degree-of-freedom system, as illustrated in Fig. 2 (a). The translational movement of the pile-cap is assigned as the first degree of freedom (DOF), and the translational movement of the superstructure is assigned as the second DOF. The lateral pushover analysis of the two-degree-of-freedom bridge bent is performed by applying an incremental lateral load V_s at the superstructure and an incremental lateral load V_{pc} at the pile-cap. The correlation between the incremental lateral forces V_{pc} and V_s can be determined using the modal analysis approach recommended by ATC-40 [1]. For the i^{th} vibration mode of a multiple degree of freedom system, the modal lateral force V_{ji} applied at the degree of freedom j can be determined by the following equation [1]:

$$V_{ji} = m_j \, \phi_{ji} \, \Gamma_i \, S_a(T_i) \tag{1}$$

where m_j is the seismic mass of the degree of freedom j, ϕ_{ji} is the mode shape value of the degree of freedom j at the i^{th} mode, Γ_i is the modal participation factor of the i^{th} mode, and $S_a(T_i)$ is the spectral acceleration predicted for the period of T_i, which is the natural vibration period of the system at i^{th} mode. For a two-degree-of-freedom bridge bent, the modal participation factor of the first vibration mode Γ_1 is significantly larger than that of the second vibration mode Γ_2. Therefore, only the modal lateral forces of the first mode need to be considered for the pushover analysis. The ratio of the pushover force increment R_V is defined as the ratio between the increment of the force applied on the pile-cap δV_{pc} and the increment of the force on the superstructure δV_s. The force increment ratio R_V can be determined by the following equation [11]:

$$R_V = \frac{\delta V_{pc}}{\delta V_s} = \frac{m_f \phi_{11}}{m_s \phi_{21}} = \frac{2 m_f}{m_s(\lambda_b + \lambda_c)} \tag{2}$$

where m_s is the seismic mass of the superstructure, m_f is the seismic mass of the pile-cap, and λ_b and λ_c are coefficients related to both the mass and stiffness of the bridge and foundation. The coefficients λ_b and λ_c are defined as $\lambda_b \equiv \beta_k - \beta_m + 1$ and $\lambda_c \equiv \sqrt{\beta_k^{\,2} - 2\beta_k(\beta_m - 1) + (\beta_m + 1)^2}$, where $\beta_m \equiv m_f / m_s$ is the mass ratio, and β_k is the stiffness ratio. The stiffness ratio is defined as the ratio between the stiffness of the foundation K_f and the stiffness of the column K_s, that is, $\beta_k \equiv K_f / K_s$ [11]. It is worth to note that the column stiffness decreases from K_{s1} to K_{s2} after the formation of the plastic hinge in the column. Similarly, the foundation stiffness decreases from K_{f1} to K_{f2} after reaching its yield limit state. Consequently, the stiffness ratio β_k changes after the column or the foundation reaches its effective yield limit state. Thus, the pushover force increment ratio R_V must be adjusted to account for the effect of significant changes in lateral stiffness. In the pushover process, the bridge bent is pushed up to a displacement corresponding to its performance limit. At this limit, the inelastic deformation of the column reaches the *damage-control* limit state, or the inelastic deformation of the piles reaches the *serviceability* limit state, whichever occurs first.

The load-displacement curve of the bridge bent at a scour depth of $L_a = 0$ m is plotted in Fig. 4(a) to illustrate the result of the pushover analysis. The lateral load V_T in the figure is the summation of the lateral force applied at the superstructure V_s and that applied at the pile-cap V_f, that is, $V_T = V_f + V_s$. The lateral displacement employed for the figure is the displacement of the superstructure Δ_s. The points corresponding to the yield limit state and the *damage-control* limit state of the column are also noted in Fig. 4(a). When the bridge bent with $L_a = 0$ m is subjected to lateral loads, inelastic deformation only develops in the column; the performance limit of the bridge bent is the *damage-control* limit state of the column. Therefore, prior to river scouring, the foundation has sufficient strength to protect itself from any inelastic deformation during an earthquake. The load-displacement curve of the bridge bent at a scour depth of $L_a = 4.5D_p = 4.5\,m$ is plotted in Fig. 4(b). When the bridge bent with $L_a = 4.5D_p$ is subjected to lateral loads, the foundation reaches its yield limit state first and is immediately followed by the yield limit state of the column. The yielded column largely limits the lateral force imposed from the inertia of the superstructure onto the foundation. However, the foundation still reaches its *serviceability* limit state because the *serviceability* limit is very close to the effective yield limit state of the foundation. The seismic performance of the bridge is controlled by the foundation when the scour depth is equal to $L_a = 4.5D_p$.

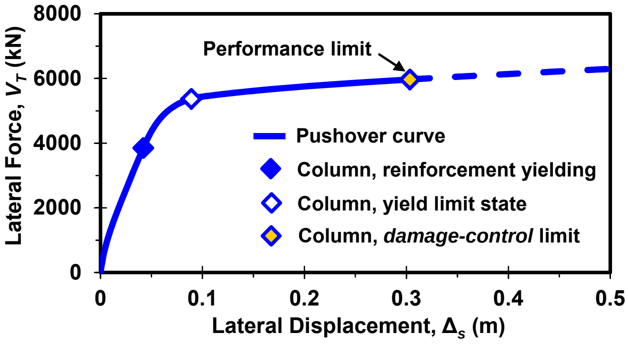

(a)

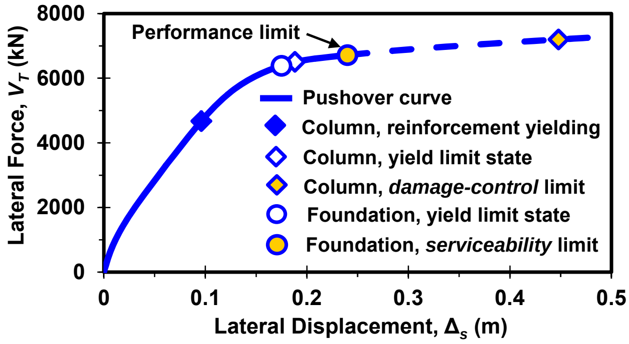

(b)

Fig. 4 – Load-displacement curve of the bridge bent at a scour depth of (a) $L_a = 0$ m, and (b) $L_a = 4.5$ m.

3.3 Capacity Spectrum, and Spectral Acceleration and Spectral Displacement at Performance Limit

The load-displacement curves of the bridge bent is converted to capacity spectrum using the approach recommended by ATC-40 [1]. The capacity spectrum is plotted in the spectral acceleration S_a vs. spectral displacement S_d format. In the capacity spectrum, the spectral acceleration S_a can be calculated from the lateral force V_T of the load-displacement curve using the following equation [1]:

$$S_a = \frac{V_T}{\alpha_1 (m_s + m_f) g} \tag{3}$$

where m_s is the seismic mass of the superstructure, m_f is the seismic mass of the pile-cap, and α_1 is the modal mass coefficient of the first mode. The modal mass coefficient α_1 is calculated by the following equation [11]:

$$\alpha_1 = \frac{(2\beta_m + \lambda_b + \lambda_c)^2}{(\beta_m + 1)[4\beta_m + (\lambda_b + \lambda_c)^2]} \tag{4}$$

where β_m is the mass ratio, and λ_b and λ_c are coefficients related to the mass ratio β_m and stiffness ratio β_k. The spectral displacement S_d is related to the displacement of the superstructure Δ_s by the following equation [1]:

$$S_d = \frac{\Delta_s}{\Gamma_1 \phi_{21}} \tag{5}$$

where Γ_1 is the modal participation factor of the first mode, and ϕ_{21} is the mode shape value of the superstructure displacement in the first mode. By assuming the mode shape value $\phi_{21} = 1$, the modal participation factor of the first mode can be determined as follows [11]:

$$\Gamma_1 = \frac{(\lambda_b + \lambda_c)(2\beta_m + \lambda_b + \lambda_c)}{4\beta_m + (\lambda_b + \lambda_c)^2} \tag{6}$$

The modal mass coefficient α_1 in Eq. (4) and the modal participation factor Γ_1 in Eq. (6) require the determination of the coefficients λ_b and λ_c, which are dependent on the ratio between the stiffness of the foundation K_f and that of the column K_s. In a nonlinear structural system, the effective stiffness (secant stiffness) should be used to determine the modal mass coefficient α_1 and the modal participation factor Γ_1 [1]. In the present study, the modal mass coefficient α_1 and the modal participation factor Γ_1 are calculated using the the secant stiffness at each point of the load-displacement curves of the column and foundation.

Table 3 – Governing performance limit states, spectral displacements, spectral accelerations, and effective vibration periods at different scour depths.

Scour depth	Performance limit	S_{dP} (m)	S_{aP} (g)	T_{eP} (s)
$L_a = 0D_p$	Column, *Damage-control*	0.271	0.652	1.29
$L_a = 2D_p$	Column, *Damage-control*	0.290	0.666	1.32
$L_a = 4.07D_p$	Column, *Damage-control*	0.362	0.669	1.47
$L_a = 4.08D_p$	Foundation, *Serviceability*	0.361	0.669	1.47
$L_a = 4.5D_p$	Foundation, *Serviceability*	0.225	0.615	1.21
$L_a = 5D_p$	Foundation, *Serviceability*	0.188	0.576	1.15

After constructing of the capacity spectrum, the spectral displacement S_{dP} and spectral acceleration S_{aP} at the performance limit of the bridge bent can be determined. Table 3 summarizes the governing performance limit states, spectral displacements S_{dP}, and spectral accelerations S_{aP} at different scour depths. For a scour depth less than $L_a = 4.07D_p$, the spectral displacement S_{dP} and spectral acceleration S_{aP} increase as the scour depth increases. The performance limit of the bridge bent is the *damage-control* limit state of the column. After the scour depth exceeds $L_a = 4.08D_p$, the performance limit of the bridge bent changes to the *serviceability* limit state of the foundation. The spectral displacement S_{dP} and spectral acceleration S_{aP} decrease with increasing scour depth.

In the capacity spectrum, each point of (S_d, S_a) is correlated to an effective vibration period T_e. At the performance limit of the bridge, the correlation between the effective vibration period T_{eP}, spectral acceleration S_{aP}, and spectral displacement S_{dP} is given as follows:

$$T_{eP} = 2\pi\sqrt{\frac{S_{dP}}{S_{aP}}} \tag{7}$$

Table 3 also summarizes the effective vibration periods T_{eP} at the performance limit of the bridge for different scour depths. The effective vibration period T_{eP} increases with increasing scour depth, when the performance limit state of the bridge remains to be the *damage-control* limit of the column. However, the effective vibration period T_{eP} decreases with increasing scour depth, when the performance limit state of the bridge changes to the *serviceability* limit of the foundation. The spectral acceleration and displacement at the performance limit of the bridge are essentially dependent on the global capacity of the bridge bent. This set of spectral acceleration and displacement is further utilized to calculate the level of seismic demand required to cause the bridge to reach its performance limit.

3.4 Effective Damping at Performance Limit

The damping of a structural system has a significant influence on the magnitude of the structure's response during an earthquake. Therefore, an assessment of the seismic demand associated with the performance limit of a bridge requires an estimation of the equivalent damping ratio at the performance limit being considered. For a yielded structural system, the equivalent damping ratio ζ_{eq} is conventionally taken as the combination of the elastic damping ratio ζ_{el} and a modified hysteretic damping ratio $\kappa \times \zeta_{hyst}$ under an inelastic response [1]:

$$\zeta_{eq} = \zeta_{el} + \kappa\zeta_{hyst} \tag{8}$$

where κ is the damping modification coefficient, which is discussed later in this section. In Eq. (8), the elastic damping ratio ζ_{el} represents the viscous damping inherent in the soil-structure system prior to reaching its effective yield limit state. For the bridge bent shown in Fig. 1, the compliance of the surrounding soil gives the foundation system an elastic damping ratio that is higher than that of the column and the superstructure. The soil-structure system actually consists of two subsystems with different levels of elastic damping. In this case, the elastic damping ratio of the soil-structure system at its first vibration mode can be calculated using an equation originally proposed for base-isolated bridges [12] and later adopted in soil–structure interaction analyses [11]:

$$\zeta_{el} = \frac{4\beta_k\zeta_f + (\lambda_b + \lambda_c - 2)^2 \zeta_s}{4\beta_k + (\lambda_b + \lambda_c - 2)^2} \tag{9}$$

where β_k is the stiffness ratio of the bridge bent, λ_b and λ_c are the coefficients related to the mass and stiffness of the bridge bent, ζ_f is the damping ratio of the soil-foundation system, and ζ_s is the damping ratio of the column and superstructure. The stiffness ratio β_k used to estimate the elastic damping ratio ζ_{el} in Eq. (9) must be calculated from the elastic stiffness of the foundation and the column, that is, $\beta_k = K_{f1}/K_{s1}$. In this study, the damping ratio of the soil-foundation system is assumed to be $\zeta_f = 15\%$, based on the conclusion of a series of experiments presented in Reference [13]; the damping ratio of the reinforced concrete column is taken as $\zeta_s = 5\%$.

The hysteretic damping ratio ζ_{hyst} in Eq. (8) is related to the energy absorbed within one cycle of inelastic response, which is loaded up to the performance limit of the bridge. Guidance to assess the hysteretic damping ratio using the nonlinear load-displacement relation is available in literature [10]. In the present study, the approach provided in ATC-40 [1] is adopted to determine the hysteretic damping ratio at the performance limit of the bridge using the capacity spectrum. The capacity spectrum is idealized to a bilinear relation with a linear elastic line that passes through the first yield point. The post-yield line is defined by connecting the point corresponding to the performance limit, that is, (S_{dP}, S_{aP}), to the equivalent yield point (S_{dY}, S_{aY}) of the bilinear idealization. The equivalent yield point is determined by equating the area under the nonlinear capacity spectrum to the bilinear idealization. The hysteretic damping ratio ζ_{hyst} at the performance limit can be calculated by the followings [1]:

$$\zeta_{hyst} = \frac{0.637(S_{aY}S_{dP} - S_{dY}S_{aP})}{S_{aP}S_{dP}} \tag{10}$$

When a structure is subjected to a long-duration earthquake excitation, the hysteretic loop may not be as perfect as assumed in the development of Eq. (10) [1]. A damping modification factor κ is introduced to Eq. (8) to account for the reduction of the hysteretic damping ratio ζ_{hyst} in an imperfect hysteresis loop. For a ductile structure subjected to a long-duration earthquake excitation, the damping modification factor κ is given by the following [1]:

$$\kappa = \begin{cases} 0.67 & \text{for } \zeta_{hyst} \le 25\% \\ 0.845 - \dfrac{0.446(S_{aY}S_{dP} - S_{dY}S_{aP})}{S_{aP}S_{dP}} & \text{for } \zeta_{hyst} > 25\% \end{cases} \tag{11}$$

Equation (11) shows that a 33% reduction is assumed for $\zeta_{hyst} \le 25\%$. A greater level of reduction is required when the structure is subjected to a larger inelastic deformation, and the hysteretic damping ratio ζ_{hyst} given by Eq. (10) is greater than 25%.

3.5 Seismic Demand at Performance Limit

Upon the determination of the spectral acceleration S_{aP}, effective vibration period T_{eP}, and equivalent damping ratio ζ_{eq} at the performance limit of the bridge, the level of the seismic demand required to reach this performance limit can readily be assessed using the approach provided in FEMA-P750 [14]. This approach must first find the bridge site's mapped spectral response acceleration parameters S_S and S_1 for short periods and the $1\,\text{s}$ period, respectively. For the given mapped spectral response acceleration parameters, the short-period site coefficient F_a and long-period site coefficient F_v can be selected based on the soil profile classification of the bridge site as per FEMA-450 [2]. At this point, the peak ground acceleration required for the bridge to reach its performance limit, denoted as PGA_P, can be determined from the spectral acceleration S_{aP} and effective vibration period T_{eP} using the following equation [2]:

$$PGA_P = \begin{cases} \dfrac{B_D}{2.5} S_{aP} & 0.2T_S \le T_{eP} < T_S \\ \dfrac{B_D T_{eP}}{2.5 T_S} S_{aP} & T_S \le T_{eP} \end{cases} \tag{12}$$

where $T_S \equiv (F_v S_1)/(F_a S_S)$ is the period that delineates the acceleration-controlled and velocity-controlled regions in the response spectrum, and B_D is the damping effect coefficient to assess the spectral response under an equivalent damping ratio of ζ_{eq}. The correlation between the damping coefficient B_D and the damping ratio ζ_{eq} is available in FEMA-450 [2].

The demand spectrum correlated to the performance limit of the bridge is determined using the peak ground acceleration PGA_P. The demand spectrum is also plotted in the spectral acceleration S_a vs. spectral displacement S_d format. The spectral acceleration S_a at different effective periods T_e is calculated following the procedure given in FEMA-P750 [14]. For effective periods $T_e < 0.2T_S$, the spectral acceleration is given by $S_a = [1 + (12.5/B_D - 5)T_e/T_S]PGA_P$. For effective periods $0.2T_S \le T_e < T_S$, the spectral acceleration is $S_a = (2.5/B_D)PGA_P$. For effective periods $T_S \le T_e$, the design spectral response acceleration is given by $S_a = (2.5T_S)/(B_D T_e)PGA_P$. The correlation between the spectral displacement S_d, the spectral acceleration S_a, and the effective vibration period T_e is $S_d = (S_a T_e^2)/(4\pi^2)$. Results from the assessment of the demand spectrum are illustrated in Fig. 5. The figure shows the capacity spectrum and the demand spectrum correlated to the performance limit of the bridge at the scour depths of $L_a = 0\,m$ and $L_a = 4.5D_p = 4.5\,m$. Different symbols are used to specify the various limit states in the capacity spectrum. The yield and performance limit states of the column are plotted as diamond dots, whereas the yield and performance limit states of the foundation are plotted as circular dots in Figs. 5(a) and 5(b).

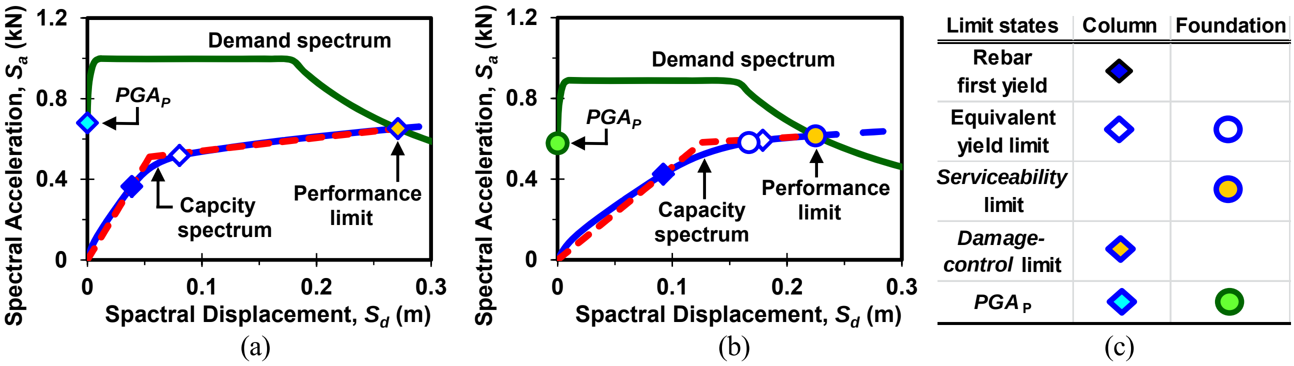

Fig. 5 – Capacity and demand spectra of the bridge bent at a scour depth of (a) $L_a = 0$ m and (b) $L_a = 4.5$ m and (c) list of the limit states.

4. Influence of Riverbed Scour on Seismic Performance

In this study, the influence of riverbed scouring on the seismic performance of a bridge is assessed by comparing the peak ground accelerations PGA_P required to reach the performance limit of the bridge at different scour depths. For the bridge bent shown in Fig. 1, the PGA_P values at different scour depths are plotted in Fig. 6. Before river scouring, that is, $L_a = 0\,m$, the seismic performance limit of the bridge is the column reaching the *damage-control* limit. The peak ground acceleration correlated to the performance limit is $PGA_P = 0.69$ g. When the scour depth is less than $L_a = 4.07D_p$, the foundation still has sufficient strength, and the seismic performance limit remains to be the *damage-control* limit of the column. The PGA_P value increases by about 17% when the scour depth increases by $4D_p$; this indicates an improved seismic performance from the riverbed scour. This improvement in seismic performance is mainly attributed to the increase of the effective vibration period T_{eP} with increasing scour depth, as shown in Table 3. After the scour depth reaches $L_a = 4.08D_p$, the foundation strength is insufficient to protect itself from being damaged by earthquake excitations. The seismic performance limit of the bridge bent changes from the *damage-control* limit of the column to the *serviceability* limit of the foundation. The peak ground acceleration PGA_P required to reach the performance limit of the bridge decreases rapidly with increasing scour depth. Figure 6 shows that the PGA_P value decreases by more than 25% with a $0.5D_p$ scour depth increase. For a scour depth greater than $L_a = 4.3D_p$, the PGA_P value is smaller than the PGA_P value at $L_a = 0\,m$. The seismic performance of the bridge is worse than that of the original design. The rate of reduction of PGA_P gradually decreases when the scour depth exceeds $L_a = 4.5D_p$.

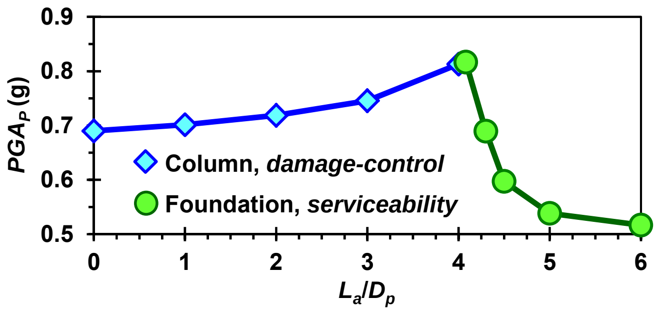

Fig. 6 – Peak ground accelerations correlated to the performance limit of a bridge at different scour depths.

5. Conclusion

Many bridges located in earthquake-prone regions also suffer from serious foundation exposure caused by riverbed scour. The loss of surrounding soil significantly reduces the lateral stiffness and strength of the foundation. This reduced stiffness and strength lead to the risk of undesirable damages to the piles during a design-level earthquake. The seismic performance of a bridge suffering from foundation exposure is likely to differ completely from that of the original bridge without foundation exposure. This study applies the capacity spectrum approach to assess the seismic performance of a bridge at different scour depths. The global capacity of the bridge is assessed based on the lateral pushover curve obtained from the 2D nonlinear finite element analysis. The bridge is idealized as a two-degree-of-freedom system with different lateral forces applied at the superstructure and pile-cap. The correlation between the lateral force applied on the pile-cap and that on the superstructure is assessed by the modal analysis of a bridge bent. The increment of the lateral force is adjusted after the bridge column or the foundation reaches its yield limit states to account for the effect of significant stiffness changes. The bridge bent is pushed up to a displacement corresponding to its performance limit. At this limit, either the inelastic deformation of the column reaches the *damage-control* limit state or the inelastic deformation of the piles reaches the *serviceability* limit state, whichever occurs first. After converting the pushover curve to the capacity spectrum, the point corresponding to the performance limit of the bridge is identified to determine the seismic demand required to reach this performance limit. In this study, the influence of riverbed scouring on the seismic performance of a bridge is assessed by comparing the seismic demands correlated to the performance limit at different scour depths. Results highlight that the seismic performance of a bridge originally equipped with sufficient foundation strength is governed by the *damage-control* limit of the column. The seismic demand correlated to its performance limit initially increases with increasing scour depth. An improved seismic performance is observed when the scour depth is shallow. However, riverbed scour reduces the lateral strength of the foundation and increases the potential of foundation damage during an earthquake. Once the scour depth exceeds a critical level, the seismic performance of the bridge is controlled by the *serviceability* limit of the foundation. The seismic demand required to reach the performance limit of the bridge decreases rapidly when the scour depth increases; this result indicates a significant decline of the seismic performance of the bridge.

6. Acknowledgements

This research was sponsored by the Ministry of Science and Technology of Taiwan, R.O.C., under Grant No. 104-2625-M-005-002. Their financial support is gratefully acknowledged.

7. References

[1] Applied Technology Council (ATC) (1996): Seismic Evaluation and Retrofit of Concrete Buildings. *ATC-40*, Applied Technology Council, Redwood City, California.

[2] National Earthquake Hazards Reduction Program (NEHRP) (2003): NEHRP Recommended Provisions and Commentary for Seismic Regulations for New Buildings and Other Structures, *FEMA 450*. Washington, D.C.

[3] Mazzoni S, McKenna F, Scott MH, Fenves GL, *et al*. (2009): Open System for Earthquake Engineering Simulation (*OpenSees*), Pacific Earthquake Engineering Research Center, University of California, Berkeley, California.

[4] Scott BD, Park R and Priestley MJN (1982): Stress-strain behavior of concrete confined by overlapping hoops at low and high strain rates. *ACI Journal*, **79**, 13-27.

[5] Mander JB, Priestley MJN and Park R (1988): Theoretical stress-strain model for confined concrete. *Journal of Structural Engineering*, **114** (8), 1804-1826.

[6] Priestley MJN, Seible F and Calvi GM (1996): *Seismic Design and Retrofit of Bridges.* Wiley- Interscience, New York.

[7] Menegotto M and Pinto PE (1973): Method of analysis for cyclically loaded reinforced concrete plane frames including changes in geometry and non-elastic behavior of elements under combined normal force and bending. *IABSE Symposium on Resistance and Ultimate Deformability of Structures Acted on by Well-defined Repeated Loads*, Lisbon, Portugal.

[8] O'Neill MW and Murchison JM (1983): An evaluation of p-y relationships in sands. *Research Report PRAC 82-41-1*, Department of Civil Engineering, University of Houston, Houston, Texas.

[9] California Department of Transportation (Caltrans) (2011): *California Amendments to AASHTO LRFD Bridge Design Specifications－Fourth Edition*. Sacramento, California, 10-84A.

[10] Priestley MJN, Calvi GM and Kowalsky MJ (2007): *Displacement Based Seismic Design of Structures*, IUSS Press, Pavia, Italy.

[11] Song ST, Wang CY and Huang WH (2015): Earthquake damage potential and critical scour depth of bridges exposed to flood and seismic hazards under lateral seismic loads. *Earthquake Engineering and Engineering Vibration*, **14** (4), 579-594.

[12] Hwang JS, Sheng LH and Gates JH (1994): Practical analysis of bridges on isolation bearings with bi-linear hysteresis characteristics. *Earthquake Spectra*, **10** (4), 705-727.

[13] Lundgreen CC (2010): Damping Ratio for Laterally Loaded Pile Group in Fine Grained Soils and Improved Soils. *Master thesis*, Brigham Young University, Provo, USA

[14] National Earthquake Hazards Reduction Program (NEHRP) (2009): NEHRP Recommended Seismic Provisions for New Buildings and Other Structures, *FEMA P-750*. Washington, D.C.